Mon. Not. R. Astron. Soc. **000**, 1–11 (2010) Printed 3 February 2010 (MN LATEX style file v2.2)

The Role of Environment on the Formation of Early-Type Galaxies

Ben Rogers[1], Ignacio Ferreras[2⋆], Anna Pasquali[3], Mariangela Bernardi[4], Ofer Lahav[5], and Sugata Kaviraj[2,6,7]

[1] *Department of Physics, King's College London, Strand, London WC2R 6LS*
[2] *Mullard Space Science Laboratory, University College London, Holmbury St Mary, Dorking, Surrey RH5 6NT*
[3] *Max-Planck-Institut für Astronomie, Königstuhl 17, D-69117 Heidelberg, Germany*
[4] *Department of Physics and Astronomy, University of Pennsylvania, USA*
[5] *Department of Physics and Astronomy, University College London, Gower St. London WC1E 6BT*
[6] *Blackett Laboratory, Imperial College London, London SW 2AZ*
[7] *Astronomy group, The Denys Wilkinson Building, Keble Road, Oxford, OX1 3RH*

MNRAS in press – arXiv version

ABSTRACT

The effect of environment on galaxy formation poses one of the best constraints on the interplay between mass assembly and star formation in galaxies. We present here a detailed study of the stellar populations of a volume-limited sample of early-type galaxies from the *Sloan Digital Sky Survey*, across a range of environments – defined as the mass of the host dark matter halo, according to the groups catalogue of Yang et al. The stellar populations are explored through the SDSS spectra, via projection onto a set of two spectral vectors determined from Principal Component Analysis. This method has been found to highlight differences not seen when using standard, model-dependent comparisons of photo-spectroscopic data. We find the velocity dispersion of the galaxy to be the main driver behind the different star formation histories of early-type galaxies. However, environmental effects are seen to play a role (although minor). Our Principal Components allow us to distinguish between the effects of environment as a change in average age (mapping the time lapse of assembly) or the presence of recent star formation (reflecting environment-related interactions). Galaxies populating the lowest mass halos have stellar populations on average $\sim$1 Gyr younger than the rest of the sample. The fraction of galaxies with small amounts of recent star formation is also seen to be truncated when occupying halos more massive than $\mathrm{M_H} \gtrsim 3\times10^{13}\mathrm{M_\odot}$. The sample is split into satellite and central galaxies for a further analysis of environment. Small but measurable differences are found between these two subsamples. For an unbiased comparison, we have to restrict this analysis to a range of halo masses over which a significant number of central and satellite galaxies can be found. Over this mass range, satellites are *younger* than central galaxies of the same stellar mass. The younger satellite galaxies in $\mathrm{M_H} \sim 6\times10^{12}\mathrm{M_\odot}$ halos have stellar populations consistent with the central galaxies found in the lowest mass halos of our sample (i.e. $\mathrm{M_H} \sim 10^{12}\mathrm{M_\odot}$). This result is indicative of galaxies in lower mass halos being accreted into larger halos.

Key words: methods: statistical – galaxies: elliptical and lenticular, cD – galaxies: evolution – galaxies: formation – galaxies: halos.

1 INTRODUCTION

The origin and evolution of early-type galaxies is a long debated topic, its solution involving a large array of cosmological and astrophysical processes. The current paradigm of galaxy formation is embedded in the ΛCDM cosmology, from which the structures in the Universe are built hierarchically. Under this framework, early-type galaxies are effectively a secondary stage in galaxy evolution. The first stage consists of the formation of rotationally-supported disk galaxies, built up through the accretion of gas and smaller systems. Mergers subsequently operate, creating early-type galaxies. The masses and ages of the stellar populations in early-type galaxies imply that these systems are the result of an intense starburst, followed by processes which quench star formation after which the galaxy evolves passively.

One of the proposed mechanisms to stop star formation requires the removal of gas from the galaxy, involving either fast removal of cold gas (ram-pressure stripping), or a slower removal

⋆ E-mail: ferreras@star.ucl.ac.uk

of hot diffuse gas (strangulation). These mechanisms, however, do not result in a change in kinematics and only minor changes in morphology (Weinmann et al. 2009) and so they can possibly explain the increased fraction of S0 galaxies (e.g. Dressler 1980). The major formation process of red sequence galaxies is thought to operate through major mergers (e.g. De Lucia et al. 2006) which result in the required structural and dynamical changes. Such processes have been known for a considerable time to produce spheroidal galaxies (Toomre & Toomre 1972; Barnes & Hernquist 1996; Khochfar & Burkert 2003),as well as more detailed photometric and dynamical properties (Naab & Burkert 2003, 2006). More recent results also suggest that minor mergers may play an increasingly important role in the build up and size evolution of massive ellipticals at relatively later times (e.g. Khochfar & Silk 2006; Bezanson et al. 2009; Bernardi et al. 2009). The subsequent quenching of star formation and evolution of the galaxy onto the red sequence, requires the gas to be removed or heated to prevent the formation of new stars. Currently models invoke feedback from active galactic nuclei (AGN), since this fits naturally into the merger scenario. Such interactions are expected to drive material to the centre of the galaxy through tidal torques, towards the central supermassive black hole (SMBH) (di Matteo et al. 2007). The discovery of a correlation between the mass of the SMBH and galaxy mass (Gebhardt et al. 2000), put significant weight behind the idea and provided scope for more comprehensive theories (Hopkins et al. 2006; Faber et al. 2007; Somerville et al. 2008).

This scenario naturally introduces an expectation of environmental dependence, since such formation process involves interactions with neighbouring galaxies and structures. A correlation with environment can arise in two forms. Firstly through the initial conditions, as these provide the impetus for the formation of the first galaxies so that objects in dense environments will form earlier than in average or low density regions (Gottlöber et al. 2001; Berlind et al. 2003). Secondly, in higher density regions interactions, mergers, gas stripping, etc, are more likely to take place over the lifetime of a galaxy and so galaxies in these environments will be pushed onto the red sequence at earlier times. Certainly the fact that red early-type galaxies are preferentially found in higher density environments (e.g. Dressler 1980; Blanton et al. 2005; Weinmann et al. 2006), suggests that environment plays an important role in their evolution. Therefore, looking at environmental differences in the stellar populations of early-type galaxies offers a method by which to constrain their formation.

There has been much work on studies of differences in stellar populations through many different methods; the variations in the tight correlations followed by the early-type population such as the colour magnitude relation (see e.g. Gallazzi et al. 2006) and the fundamental plane (see e.g. Bernardi et al. 2003), galaxy colours (see e.g. Blanton et al. 2005), absorption line indices (see e.g. Nelan et al. 2005) and the parameters of population synthesis modelling (see e.g. Bernardi et al. 2006; Thomas et al. 2005). In all cases the effect of environment has been shown to be relatively weak, if observed at all. Thus we take a different approach, choosing a different methodology involving principal component analysis on spectral data to identify small differences between the stellar populations of early-type galaxies (Rogers et al. 2007), in a similar style to Ferreras et al. (2006), over a range of environments.

The environment is in most cases quantified through the projected number density of galaxies, typically the distance to the n^{th} nearest neighbour. However it has been argued that more physically motivated scales of environment are the mass and the virial radius of the host dark matter halo (Kauffmann et al. 2004; Yang et al. 2005; Weinmann et al. 2006; Blanton & Berlind 2007) . Not only are environmental dependencies observed to act primarily over distances comparable to the virial radius of such halos (Goto et al. 2003), but also the merger history of the dark matter halo is determined mainly by its present mass (Kauffmann et al. 2004). The mass of the host dark matter halo cannot be directly measured in most cases but can be estimated through galaxy group catalogues (e.g. Yang et al. 2007). Such catalogues also provide the halo-centric radius and can be used to easily separate the sample into central and satellite populations. The other advantage in estimating the environment through halo mass is that it allows a direct comparison between observations and theoretical models. Dekel & Birnboim (2006), Somerville et al. (2008), Cattaneo et al. (2008) or Khochfar & Ostriker (2008) all make model predictions of the evolution and properties of galaxies in terms of the dark matter halo mass. For example Cattaneo et al. (2008), following the work of Birnboim & Dekel (2003) and Dekel & Birnboim (2006), suggested that the downsizing observed in elliptical galaxies can be modelled by considering a critical mass halo above which gas cannot be accreted efficiently, being shock heated to the virial temperature, thus effectively shutting down star formation.

This paper is structured as follows: we describe the sample of early-type galaxies used in this study as well as the details of the principal component analysis. We investigate the results of the PCA projections over a range of halo mass and velocity dispersion, we highlight the differences observed and investigate them using the stellar population models of Bruzual & Charlot (2003). The sample is finally split into central and satellite galaxies, whose properties are compared. The satellite population is then used to determine a possible dependence on halo-centric radius.

2 THE SAMPLE

This work is based on the large sample of early-type galaxies of Rogers et al. (2007). This sample is selected from the Bernardi et al. (2006) catalogue, compiled from the Sloan Digital Sky Survey (SDSS, York et al 2000), Data Release 4 (Adelman-McCarthy et al. 2006). It is a volume-limited sample within z$\leqslant$0.1 and $M_r \leqslant -21$. A cut with respect to signal to noise ratio (S/N) was also imposed, rejecting those spectra with S/N$\leqslant$15. The final sample comprises 7,134 early type galaxies. Here we extend Rogers et al. (2007) to investigate the effect of environment in more detail, including the information of the host dark matter halo for each galaxy, a explained below.

We make use of the Galaxy Groups Catalogue of Yang et al. (2007), which is an improved application of the Yang et al. (2005) halo-based galaxy group finder to the New York University Value-Added Catalogue (Blanton et al. 2005), based on the Sloan Digital Sky Survey Data Release 4 (York et al 2000). We cross correlate this catalogue with the original sample to find halo masses for all but 175 galaxies, leaving a total of 6,959 galaxies in the new sample used here. We have also removed a small (~ 150) set of galaxies with velocity dispersions below 125 km/s, as these galaxies only appear in the bin with the lowest halo masses, and have no counterparts in more massive halos. Allowing them to be part of the lowest velocity dispersion bin would considerably reduce the average σ in this bin, introducing a bias when compared to other halo masses.

The galaxy group finder, described in Yang et al. (2005) and Yang et al. (2007), is an iterative process in which the membership of the groups and the relationships between the properties of the halo are refined at each step. Initially the group finder uses a friends

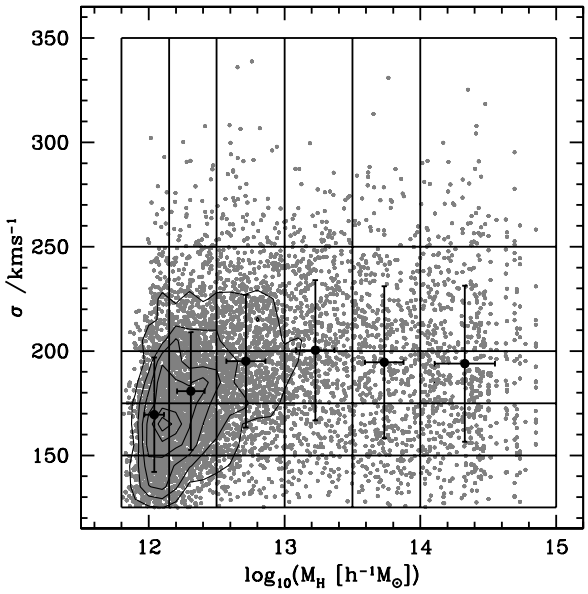

Figure 1. Our sample of SDSS early-type galaxies is shown with the two main parameters that are used to characterise the intrinsic (velocity dispersion; σ) and environmental (host halo mass; $\mathrm{M_H}$) dependence of the underlying stellar populations. In the crowded regions of the figure, contour lines track the density of galaxies in the plot. The grid corresponds to the binning applied throughout the paper. The large black dots and error bars give the average and RMS within each bin in halo mass.

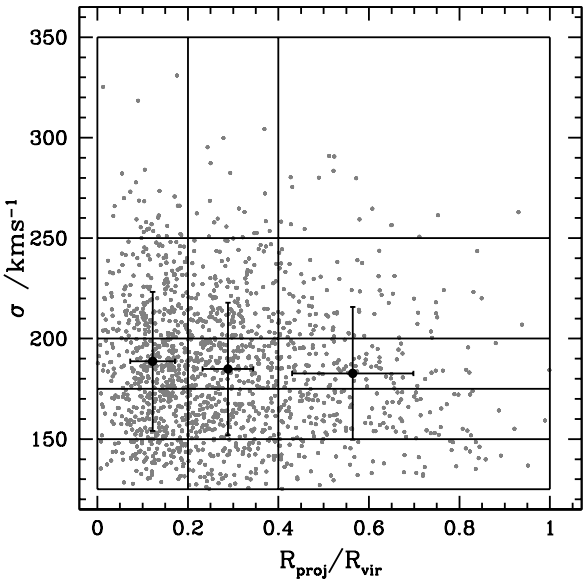

Figure 2. The projected radial distance from the luminosity-weighted centre of the group is shown with respect to velocity dispersion. The distance is scaled to the virial radius, as determined from the properties of the halo. The grid overlaying the sample shows the binning applied in the analysis. Black dots and error bars correspond to the average and RMS scatter of the sample within the bins in $\mathrm{R_{proj}}$.

of friends algorithm with small linking lengths to identify the centres of possible galaxy group candidates. In such groups the centre of the halo is given by the luminosity-weighted centre. The remaining isolated galaxies not associated with groups are also set as the potential centres of groups. The characteristic luminosity ($\mathrm{L_{19.5}}$) of each candidate group is then estimated, where this is defined as the summation of the luminosity of all group members with ${}^{0.1}\mathrm{M}_r - 5\log h \lesssim -19.5$ [1]. The $\mathrm{L_{19.5}}$ values are corrected for survey completeness and the apparent magnitude limit of the survey at redshifts z$\geqslant$0.09.

Using the characteristic luminosity, the mass of the group halo is estimated from a group mass-to-light ratio. The ratio used is set at a constant value across all groups for the first iteration but is subsequently refined to be group mass dependent. However, the results are not particularly sensitive to the exact value of the ratio even if it is held fixed (Yang et al. 2005). The estimate of the group halo mass allows the derivation of other group halo properties such as the halo radius, within which the halo has an average density contrast of 180, and the virial radius, defined as the radius within which the average density is above a set value. Once the properties of the halo have been estimated, a NFW profile is used for the dark matter (Navarro, Frenk & White 1997) to determine the three dimensional density contrast of the halo in redshift space. Further galaxies are subsequently assigned to the galaxy group candidates if they are within a certain distance of the centre. This process – which allows for the merging of two groups if all members satisfy the above criteria singularly – is repeated until the membership of each group remains constant. The final dark matter halo mass is then estimated from a linear relationship with respect to stellar mass, derived from semi-analytic models (Kang et al. 2005). The galaxy group differentiates between central and satellite galaxies. Those galaxies which are the most massive galaxy of the group are defined as centrals, whereas the remaining galaxies are labelled as satellites. Low mass halos can consist of a single, central galaxy. Shown in figure 1 is the entire sample as a function of host halo mass, $\mathrm{M_H}$, and central velocity dispersion, σ, of the individual galaxies. The black dots correspond to the average and RMS scatter of the sample, within the halo mass bins shown by the grid.

We can see from the figure that within the lowest halo mass bin ($\mathrm{M_H} \sim 10^{12}h^{-1}\mathrm{M}_\odot$) there is a limitation imposed by the size of the halo on the highest sigma galaxy that it can contain. This is similar to that seen in the main catalogue in reference to the maximum stellar mass (see e.g. Yang et al. 2008). The difference here is the non-trival mapping of velocity dispersion to dynamical or stellar mass, which is dependent on other factors such as structure. However note that since the results presented in this paper are consistent across the range of velocity dispersions considered, the details of such mapping would be unlikely to affect them. Also we are using velocity dispersion as a measure of the intrinsic properties of the galaxy, which is consistent with many stellar population studies in the literature (e.g. Bernardi et al. 2003; Gallazzi et al. 2005).

The figure also reveals a shift towards decreasing velocity dispersion at lower halo mass, whereby less massive halos on average contain smaller galaxies. This effect is illustrated by the solid circles and error bars in figure 1 which represent the average and root mean square deviation of the velocity dispersion within each bin of halo mass.

This correlation between mass / luminosity and environment in terms of halo mass (van den Bosch et al. 2008a) but also seen

[1] ${}^{0.1}M_r$ is the SDSS-r band magnitude for which K and E corrections are applied at redshift z=0.1

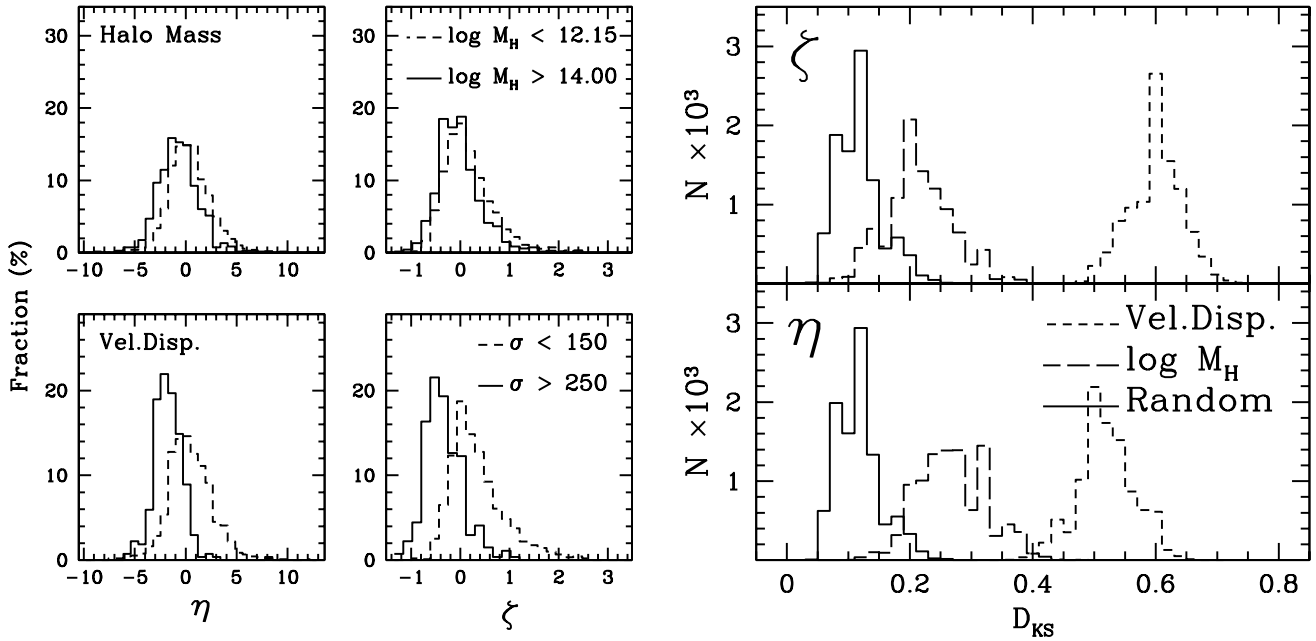

Figure 3. *Left:* Distribution in PCA components η and ζ of the upper and lower bins in velocity dispersion (*bottom*, labelled in km/s) and host halo mass (*top*, labelled in $\log(\mathrm{M}/\mathrm{M}_{\odot})$) of the entire sample in η and ζ. *Right:* distribution of the KS statistic (D_{KS}) for the subsamples of the same bins in velocity dispersion (dashed) and halo mass (long-dashed) for η (*Bottom*) and ζ (*Top*). In order to quantify the statistical significance of the segregation, the result of drawing subsamples at random over all mass ranges and environments is shown (solid).

with respect to galaxy density (Blanton et al. 2005; Croton et al. 2005), means that it is important to take into consideration how such intrinsic properties change as a function of environment. It is well known that the stellar populations of a galaxy are related to its velocity dispersion (Kauffmann et al. 2004; Thomas et al. 2005; Gallazzi et al. 2005), therefore such a correlation can generate spurious environmental effects. Hence, in order to carry out a robust analysis, it is important to separate out the effects of environment, from those that are caused by this selection bias.

To achieve this, we investigate the difference with respect to environment only at the same σ range. Our sample is divided into sub-samples either with respect to halo mass, or velocity dispersion. This classification is shown as a grid in figure 1. The choice of the grid size is motivated by the density of the underlying sample, selecting larger bins at high mass.

We also consider the variation in the properties of stellar populations with respect to the position of a (satellite) galaxy within its host halo. The dependence is measured as a function of the projected distance from the luminosity weighted centre of the group, namely the projected halo-centric radius, R_{proj}. This will allow us to assess the effect of galaxy accretion in groups on the star formation history. We expect galaxies on the outskirts of a group to be newer members. Hence, these galaxies will be increasingly subject to the various effects of the group environment, such as 'strangulation', 'ram-pressure stripping' and 'harassment' which act on the satellite galaxies of the groups (Weinmann et al. 2006; van den Bosch et al. 2008a,b). Shown in figure 2 is the satellite-only sample as a function of projected distance scaled by $\mathrm{R}_{\mathrm{vir}}$. Similar studies of satellites have found a radial mass segregation within groups (van den Bosch et al. 2008a), with the least massive galaxies at the outskirts of the group. We find no such trend within our sample with respect to velocity dispersion.

3 THE STELLAR POPULATIONS OF DIFFERENT HALO MASSES

Regarding the effect of environment on the stellar populations of elliptical galaxies, it is important to notice that the reported differences have generally been small. For example, studies of the colour-magnitude relation have only found limited and statistically weak evidence (Bernardi et al. 2003; Gallazzi et al. 2006), even more comprehensive analyses (Clemens et al. 2006; Bernardi et al. 2006) find difference of the order $\sim$ 1 Gyr. In this paper we optimise the extraction of differences from spectroscopic data via principal component analysis, which has been shown to succeed in detecting differences within highly homogeneous samples (e.g. Ferreras et al. 2006; Rogers et al. 2007).

3.1 PCA

Principal Component Analysis (PCA) is a multivariate technique that reduces the dimensionality of a data set. In most cases this is just used as a data compression algorithm. However, previous work (Madgwick et al. 2003; Ferreras et al. 2006; Rogers et al. 2007) has shown that vital information can be extracted from the projections on to the first few principal components. In this work the variables that describe the data set are the flux values at each wavelength i.e. the spectra. The task of PCA is to generate a set of basis vectors (the principal components) from the data set, such that one can rank these vectors with respect to the variance they capture. Hence, when obtaining the "coordinates" of each galaxy by projecting their spectra on to the principal components, one can use just the very few coordinates that correspond to the principal components with the highest variance. In Rogers et al. (2007) we find that the first two components already hold valuable information regarding the average age of the stellar populations and the presence

of recent star formation. We refer the reader to that paper for a detailed description of the methodology, although a brief summary is given below.

The first principal component is found to be consistent with a typically old stellar population, showing a pronounced 4000Å break, significant metal absorption lines and limited Balmer line strengths. The second component is much bluer, with absorption lines dominated by the Balmer series. A correlation between both principal components is forced by the orthogonality inherent to PCA. When projecting onto the observed spectra, the components give a relation that represents the mass-metallicity-age correlation of early-type galaxies (e.g. Bernardi et al. 2003; Thomas et al. 2005). The extended scatter in the direction of the second component i.e. with respect to an excess of blue light, is created by recent star formation. This issue is confirmed in two ways: 1) through the application of a two component stellar population model, where we find galaxies with a higher projection onto the second principal component require a higher mass fraction in young stars (Rogers et al. 2007, 2009), 2) comparing the results of PCA with NUV photometry from GALEX: The NUV−r colour is highly sensitive to small amounts of recent star formation (Schawinski et al. 2006; Kaviraj et al. 2007). Within our sample, 'NUV bright' galaxies (NUV−r$\leqslant$4.9) present higher projections of the second principal component, compared to the sample of quiescent, 'NUV faint' galaxies (NUV−r$\geqslant$5.9). This trend between PCA and the presence of young stars is optimised by rotating the projections on the two dimensional plane spanned by PC1 and PC2, to give two new components: η and ζ. These two components can be defined as the distance along the PC1-PC2 correlation (η) and the residual of the correlation (ζ). Even though NUV is more sensitive to the presence of massive stars than optical spectra, this method is complementary to NUV studies. An advantage of using optical spectra over NUV photometry is that we can track the presence of recent star formation for a greater length of time: NUV light decays very rapidly as the most massive stars die out.

In Rogers et al. (2007) we compare the PCA projections with a number of star formation histories combined with population synthesis models and conclude that η is mainly related to the average age of the stellar populations, whereas ζ tracks the presence of recent star formation (see also Rogers 2009). This interpretation is carried over to this paper for the analysis of the effects of environment.

3.2 Stellar Mass vs Group Halo Mass

In this section we look into the dependence of the stellar properties of elliptical galaxies on both the stellar mass and the mass of the halo which the galaxy occupies. We utilise the results from PCA described above, focusing on how the average properties of the galaxy (through η) and the young stellar populations (through ζ) depend on galaxy mass or halo mass. While it is true that environment plays a major role on the number density of early-type galaxies (i.e. the morphology-density relation, Dressler 1980), here we pose a different question: "at a fixed σ, how different are the star formation histories of early-type galaxies with respect to environment?". The left panel of figure 3 shows the distribution of the first and last bins in both velocity dispersion (*bottom*) and group halo mass (*top*). The comparison reveals that in terms of the mass of the galaxy (i.e. velocity dispersion), smaller galaxies have higher values of both η and ζ indicating a younger age, most likely due to increased recent star formation, in agreement with the 'downsizing' scenario (Cowie et al. 1996). However the distributions of the two extreme bins regarding environment (*top*) show a considerably smaller divergence in terms of their η or ζ distributions. Note that the preliminary results show that those galaxies in the lowest mass halos have slightly higher values of η and ζ.

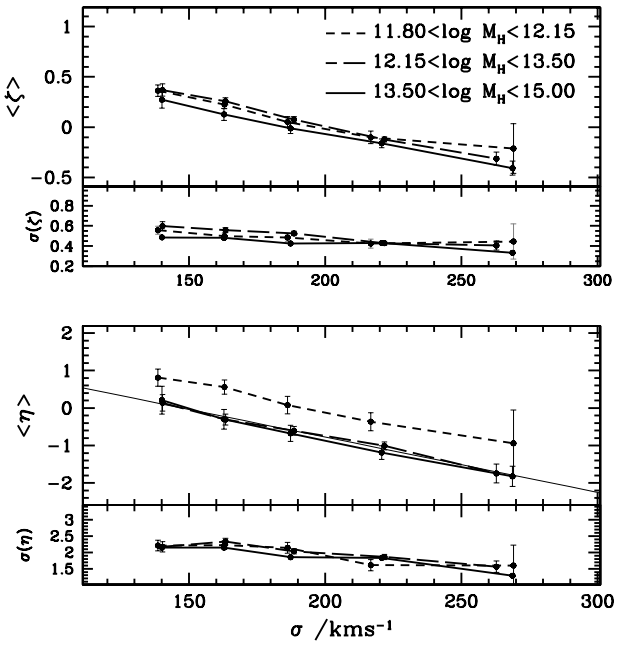

Figure 4. The average of the η and ζ components as a function of σ within each group halo mass bin, as labelled (given in $\log(M/M_\odot)$). The error bars correspond to the error on the mean. The small panels below the main plots show the standard deviation of η and ζ in each bin. The thin black line is for reference only and is a least squares fit to the three most massive halos.

The use of a Kolmogorov-Smirnov (KS) test confirms whether the galaxies in these subsamples originate from the same distribution. This is quantified in terms of the D_{KS} statistic (a measure of the maximum difference of the cumulative distributions, see e.g. Press et al. 2009). The right panel of figure 3 shows the result of a Monte Carlo simulation, where we extract samples of 100 galaxies from the upper and lower mass bins, and perform the KS test in each case. This exercise is repeated 10,000 times, and the histogram of D_{KS} is shown when extracting galaxies from the upper and lower bins in velocity dispersion (short dashed line), in host halo mass (long dashed line) of from random sampling of the complete sample (solid line). Velocity dispersion clearly plays the dominant role; its histograms in the η and ζ components are far from the distribution of random sampling. However, environment – or halo mass – plays a more subtle role, although a non-negligible one, especially with respect to the η component, which does show less of an overlap with the distribution for random sampling. Whether this effect is driven by the mass bias mentioned above or whether is it a genuine effect of environment is studied in this paper.

3.3 A detailed look at the [η, ζ] distributions

Many authors have studied the role of environment on the scaling relationships. This includes colours (e.g. Weinmann et al. 2006; Kaviraj et al. 2007), absorption line indices (e.g Kuntschner et al. 2001; Nelan et al. 2005; Bernardi et al. 2006) as well as derived quantities such as luminosity-weighted age, metallicity and $[\alpha/\mathrm{Fe}]$

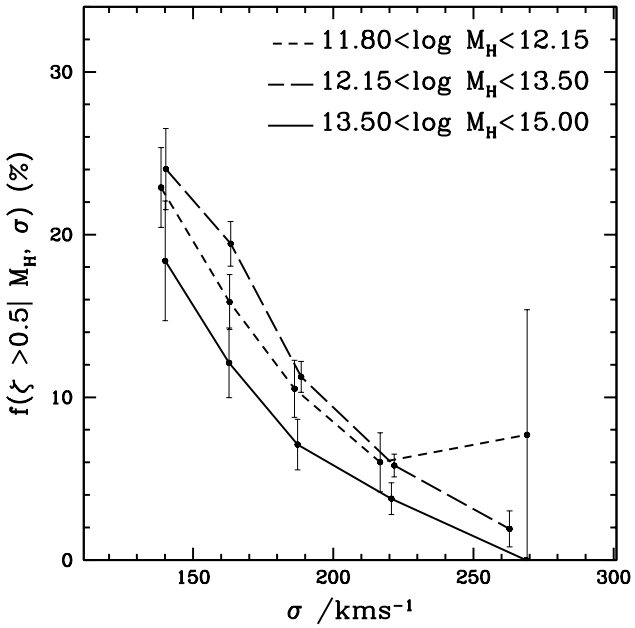

Figure 5. The fraction of galaxies with a ζ value above 0.5, which is consistent with the presence of recent star formation. Each line corresponds to a range of host halo masses, as labelled (given in $\log(\mathrm{M/M_{\odot}})$). The error bars are given by Poisson errors.

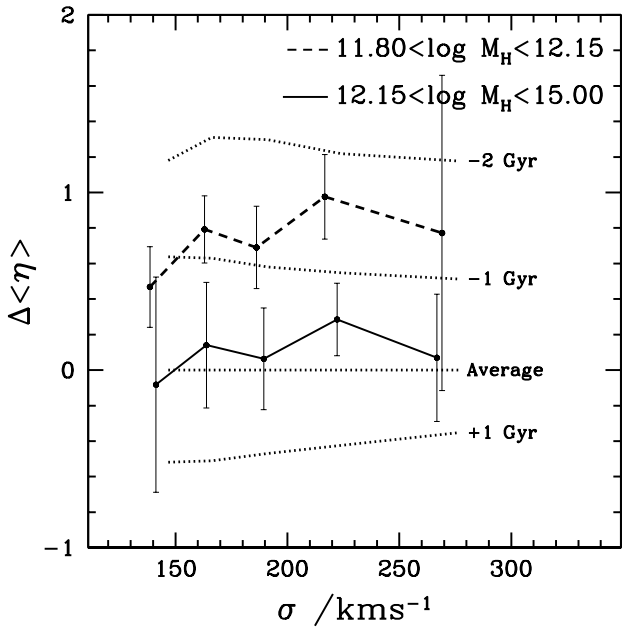

Figure 6. Change in the η component relative to the average relationship with σ via SSP fitting (see text for details). A comparison of the lowest mass halo (dashed line) to the most massive halos (solid line) is shown relative to deviations from this relationship due to an increase/decrease in the average SSP age across σ (dotted lines).

(Thomas et al. 2005; Clemens et al. 2006). In a similar vein, we extend this analysis to include the η and ζ components.

Shown in figure 4 are the average values of η and ζ with respect to velocity dispersion, for a range of host halo masses. Points corresponding to the same host halo mass range are connected. The velocity dispersion value for each bin is given by the average. A reference line is also plotted in the bottom panel. It is a least squares fit to the most massive halos and is shown in all subsequent figures of $\langle\eta\rangle$ for comparison. The error bars give the uncertainty on the mean values within each bin. The RMS deviation is shown separately at the base of each panel as $\sigma(\zeta)$ (*top*) and $\sigma(\eta)$.

A clear dependence is found with respect to velocity dispersion, such that galaxies with lower values of σ have higher components η and ζ, revealing the presence of younger stellar populations. Note that as shown in Rogers et al. (2007), principal components η and ζ are not dependent on the velocity dispersion, and so no correction is needed (in contrast with analyses of equivalent widths).

It is important to notice from figure 4 that the effect of environment is very subtle. In terms of $\langle\zeta\rangle$ and in most cases $\langle\eta\rangle$, the trends of the different host halo mass ranges are indistinguishable from each other. However, galaxies in the least massive halos show a consistent and significantly higher value of $\langle\eta\rangle$, across all values of σ (although the nature of the trend is the same for all halo mass bins). Given that the differences are small, the significance is determined through a KS test for the η component, performed by comparing galaxies in the lowest and the highest host halo bin, across all values of σ. In the three central bins of velocity dispersion we find a probability higher than 99% that the samples are drawn from different distributions. At the highest and lowest bins of σ the small number of galaxies prevent us from stating a similar result.

Furthermore, figure 4 also indicates that $\langle\zeta\rangle$ does not differentiate with respect to halo mass. This comes as a surprise, as one might have expected that recent star formation is responsible for the higher values of $\langle\eta\rangle$. To explore this issue in more detail, we use the conditional fraction of galaxies with a value of ζ above a threshold at which one needs to invoke recent star formation. We choose $\zeta \geqslant 0.5$, since galaxies above this value both require significant fractions of young stars in a two-burst model and also have NUV luminosities consistent with recent star formation (Rogers et al. 2007, 2009).

In figure 5 we show this conditional fraction as a function of velocity dispersion for a range of host halo masses. Consistent with the simple analysis performed above, the main driving force behind the fraction of galaxies with recent star formation is galaxy mass (assuming σ is representative of the mass of the galaxy). With respect to halo mass, the fraction of younger galaxies seem to split such that there is a consistent lower fraction for the most massive halo bins (black solid line) relative to the rest of the sample. The significance of this drop is not high in any one bin but the trend is notably consistent across all bins. This is a qualitatively similar result to that found in Schawinski et al. (2006) using NUV data, although here we see that recent star formation persists in halos below $\mathrm{M_H} \leqslant 3 \times 10^{13} h^{-1} \mathrm{M_{\odot}}$ and is reduced in more massive halos. The possible mechanisms underlying this effect are discussed in the conclusions.

3.3.1 Modelling the η component

We now turn to quantifying the difference in $\langle\eta\rangle$ from figure 4 through the application of stellar population synthesis models. Since the change of η is not accompanied by a change in ζ or the fractional change in high-ζ galaxies, the shift is unlikely to be related to recent star formation. Furthermore, this shift is relatively small, which implies composite models, such as an exponentially

decaying star formation history, may well blur any discriminating effect. Therefore, while the modelling of early-types can be pushed beyond relatively simple formation histories (Rogers et al. 2009), it is more robust in this case to consider simple stellar populations.

The observations are compared to synthetic spectra through the equivalent widths of absorption line indices. The model spectra are extracted from the simple stellar populations of Bruzual & Charlot (2003), using a Chabrier (2003) initial mass function. A detailed grid of models is constructed over a range of ages $\{1 \cdots 14$ Gyr$\}$ and metallicities $-1.0 \leqslant \log(Z/Z_{\odot}) \leqslant +0.35$, at solar abundance ratios. We constrain the population parameters with multiple age sensitive absorption features: Hβ, Hγ, Hδ, as well as the 4300Å absorption band (G4300) and the metallicity indicator [MgFe] (Gonzalez 2003). The absorption features are measured in each of the observed galaxy spectra, after being smoothed to the highest velocity dispersion within the respective bin. The equivalent widths (EWs) are estimated using the method outlined in Rogers et al. (2009), in which the pseudo-continuum is determined by a boosted median value of the surrounding spectrum. The specific absorption lines are targeted using a 20Å window. We use a standard maximum likelihood method to compare the observed and model absorption features. The model EWs are obtained in the same way, smoothing the spectra to the velocity dispersion considered. For each galaxy we use the probability-weighted age and metallicity, where the probability is defined as $\mathrm{P}(t, Z) \sim \exp^{-0.5\Delta\chi^2}$, which gives a robust estimate of the SSP values (e.g. Gallazzi et al. 2005). The best fits give a reduced average of $\langle\chi^2_r\rangle = 1.3$.

The average age and metallicity from each of the halo mass and velocity dispersion bins is used to investigate the difference seen in the average η value in an equivalent analysis to that shown in figure 4. However, we find no significant differences between the predicted SSP ages or metallicities with respect to host halo mass across all velocity dispersions. This illustrates the power of PCA to identify small differences in the spectra of elliptical galaxies, which might be difficult for model-based methods to identify, especially at low S/N. Therefore in order to assess the (second order) effects of environment on η, we consider small perturbations with respect to the (first order) correlation with velocity dispersion.

We define a fiducial relation between velocity dispersion and age/metallicity through the average parameters of each of the complete velocity dispersion bins i.e. including all halo masses. The SSP parameters of this relation are then offset with respect to the average age for each bin in velocity dispersion. The effect on the η component of this change (computed directly on the models) is estimated and compared to the observed values – defining for each galaxy a $\Delta\eta$ as the difference between the η value of the galaxy and that of the model corresponding to the same velocity dispersion. The model values of η are derived in the same way as for the observed values, i.e. via projection onto the principal components followed by a rotation of the projected values. This rather simple analysis enables us to quantify the change in η. Notice that we assume only a perturbation in age, as this is by far the most dominant effect reported in the literature (Bernardi et al. 2003; Thomas et al. 2005; Nelan et al. 2005).

While we are only interested in identifying the magnitude of the shift of the lowest mass halo, as a check we compare our relationship of metallicity and age with velocity dispersion to those found by other authors. We quantify this relationship through the slope of a linear fit to the fiducial relation, which was found to be: $\Delta\log(Z/Z_{\odot})/\Delta\log(\sigma) = 0.68$ and $\Delta\log(\mathrm{Age}/\mathrm{Gyr})/\Delta\log(\sigma) = 0.38$ respectively. These values are comparable to those reported in Thomas et al. (2005) (0.55, 0.24), Clemens et al. (2006)(0.76,$\sim$) and Nelan et al. (2005)(0.53,0.59).

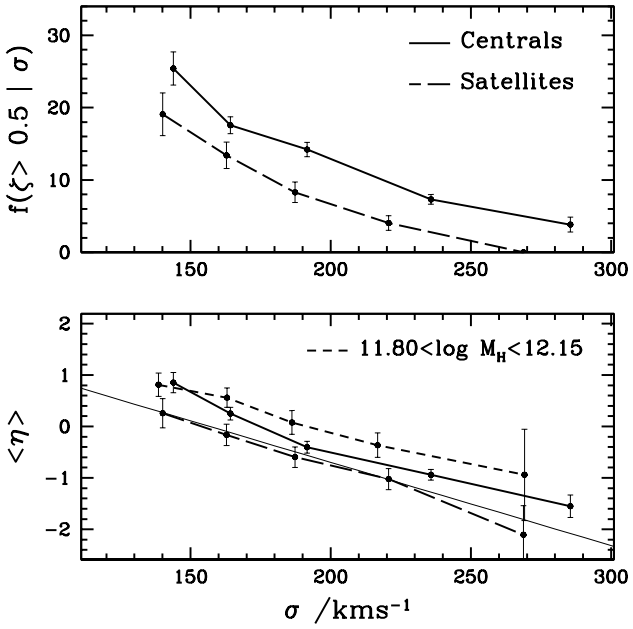

Figure 7. Comparison of the distribution of the central and satellite galaxy populations at the same velocity dispersion, with respect to average age ($\langle\eta\rangle$; *bottom*) and to recent star formation (f($\zeta \geqslant 0.5$); *top*). The short dashed line is the $\langle\eta\rangle$ for the lowest mass halo in the whole sample. The thin solid line in the bottom panel is the reference line from fig.4.

The σ vs. $\Delta\eta$ relationship is shown in figure 6 for the fiducial model obtained from the best fit SSP ages and metallicities (labelled "Average"). For reference, we also show the relation when the age is shifted by 1 or 2 Gyr as labelled. We include in the figure the observed values for the lowest halo mass (dashed line) and for the rest of the sample (thick solid line). The figure shows that early-type galaxies in the lowest density regions are on average about 1 Gyr younger than those in denser environments, a result that is consistent for a wide range of velocity dispersion. This result indicates that galaxies residing in all but the lowest mass halos have similar stellar populations suggesting they are formed in similar ways at similar redshifts. This may be due to a true invariance across average/high density environments, such that above a certain density the formation process becomes uniform.

3.4 Centrals and Satellites

The star formation histories of galaxies sitting at the centre of the dark matter halos (centrals) and galaxies which orbit around the centre (satellites) are expected to depend in a different way with respect to the mass of their host halo. Specifically, satellites are more likely to be affected by the transformation mechanisms operating in the halo environment (van den Bosch et al. 2008a,b). Therefore, we analyse separately the effects of environment on centrals and satellites and compare the relative differences.

The comparison of satellite and central early-type galaxies at the same velocity dispersion is shown in figure 7. The figure reveals that central galaxies (solid lines) have higher values of $\langle\eta\rangle$ (*bottom*) and f($\zeta > 0.5$) (*top*), indicative of younger aver-

age ages (Pasquali et al. 2009b). and significant recent star formation, respectively, when compared to satellites of the same mass (long dashed lines). This is consistent with van den Bosch et al. (2008b) and Weinmann et al. (2009), who found that in terms of optical colours, centrals are bluer than satellite galaxies, indicating younger ages. Here we can see this extends to the fraction of elliptical galaxies which harbour small amounts of recent star formation as well. However, notice that this trend includes all halo masses. In §3.4.1 we show the effect of separating this central/satellite classification with respect to halo mass.

We have also plotted in the bottom panel of figure 7 the average value of η for galaxies in the lowest mass halos (short dashed line). At the lowest halo masses all galaxies are central. Hence, this comparison allows us to rank the importance of host halo mass against the central/satellite nature. The figure shows that of these two properties, the mass of the halo dominates, i.e. centrals in low mass halos are younger than centrals in general. We focus on this aspect in the next two sub-sections.

3.4.1 Effect on average age: η

The average values of η are plotted for the two subgroups in figure 8. It is evident from the figure that the analysis is complicated by the segregation imposed naturally by the halo mass on the central/satellite nature of the galaxy. The sample lacks central galaxies in the most massive halos (a limit imposed by the survey volume). On the other hand, at a given velocity dispersion, satellites cannot be found at low halo masses (a trivial constraint imposed by the halo mass). This means a comparison of the two populations can only occur within certain ranges of halo mass. Therefore the middle panel of figure 8 shows the $\langle\eta\rangle$ values *only* over a range of halo masses in which a significant number of both centrals and satellite galaxies exist. The top and bottom panels show the central and satellite galaxies, respectively, over their full halo mass range.

The central galaxies (*top*), show an increase in the average value of $\langle\eta\rangle$ at the lowest halo masses. This is identical to the trend shown in figure 4 (notice centrals are the only type in the first halo mass bin). The result for more massive halos is consistent with the main sample. This suggests again that the effect of halo mass on the stellar populations is limited to masses below $\mathrm{M_H} \sim 10^{12}\mathrm{M_\odot}$. On the other hand, satellite galaxies (*bottom*) show an increase in $\langle\eta\rangle$ in the group halo mass range $3\times10^{12} \leqslant \mathrm{M_H} \leqslant 10^{13}\mathrm{M_\odot}$, which is the lowest halo mass bin at which significant numbers of satellite galaxies exist. The comparison in the middle panel reveals that at the overlapping halo mass i.e. $\mathrm{M_H} \sim (3\times10^{12}\cdots10^{13})\mathrm{M_\odot}$, centrals have much lower values of $\langle\eta\rangle$. Thus the increase of $\langle\eta\rangle$ found in the population of satellite galaxies would have been hidden by the dominance of centrals in this mass bin.

Given that higher η values are consistent with younger average ages suggests that satellites are in fact younger, when compared to central galaxies of the same velocity dispersion and occupying halos of similar mass (Pasquali et al. 2009b). A KS test confirms that for this halo mass range, the second and third bins in σ of the centrals and satellites are drawn from different distributions at a confidence level of $\geqslant$98% and $\geqslant$99%, respectively. While this is seemingly in contrast with the previous results, it is important to realise what is being compared in figure 8. A pure central - satellite split (as in figure 7) will generally result in a comparison of central galaxies in low richness environments with satellites in higher density regions. This is the motivation of the split in many papers, under the assumption that the centrals of today are a reasonable approximation to the progenitors of the current satellite population,

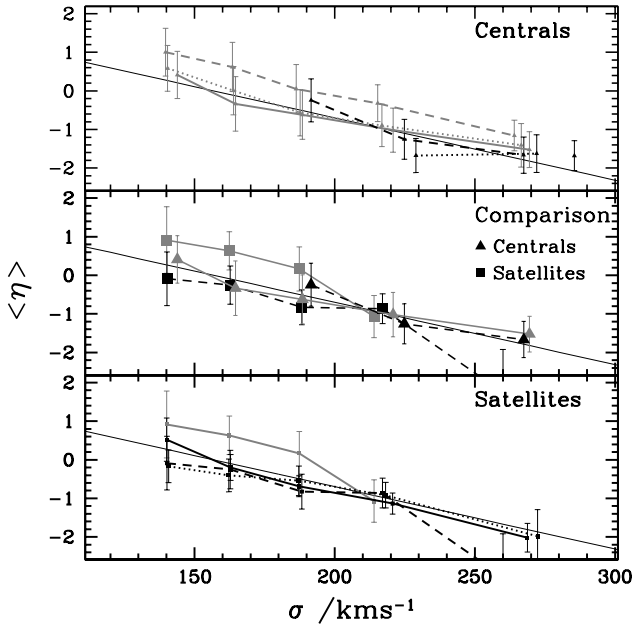

Figure 8. $\langle\eta\rangle$ values for the central and satellite galaxy populations within each bin in velocity dispersion *and* halo mass. The central panel compares central and satellite galaxies over a range of halo masses for which sufficient numbers of both types exist. The halo mass range is as follows – given in $\log(\mathrm{M_H/M_\odot})$: grey dashed(11.80,12.15); grey dotted (12.15,12.50); grey solid(12.50,13.00); black dashed (13.00,13.50); black dotted(13.50,14.00); black solid(14.00,15.00). The thin solid line shown in all panels is the reference line from fig.4.

(e.g. §4.1 van den Bosch et al. (2008b)). Here we are comparing centrals in groups of significant size, to satellites in similar groups. We find a trend in three out of the four bins considered, although it is only found to be statistically significant in two. The effect is not visible at the higher velocity dispersions.

Hence, we find that central galaxies 'evolve' faster than a similar galaxy that is accreted onto a group. This probably relates to the epochs over which environmental effects are efficient. Central galaxies within more massive halos will have interacted with other galaxies during the formation of the group and will also have existed inside a more massive halo earlier than a galaxy of the same mass which is accreted into a group halo. This result is consistent with the recent work of Bernardi et al. (2009), who found that early-type brighest cluster galaxies were $\sim$ 1Gyr older than the surrounding satellite early-type galaxies.

Figure 8 reveals that the satellite galaxies in group halos of mass $\mathrm{M_H} \sim 3\times10^{12}\cdots10^{13}\mathrm{M_\odot}$ have values of $\langle\eta\rangle$ consistent with those of the central galaxies from halos of mass $\mathrm{M_H} \sim 6\times10^{11}\cdots10^{12}\mathrm{M_\odot}$. This trend is consistent with the hierarchical build up of structures expected within the standard ΛCDM cosmology.

3.4.2 Effect on recent star formation: ζ

Figure 9 shows the fraction of galaxies with values of ζ consistent with recent star formation, with respect to central/satellite nature, in a similar manner to figure 8. The trends of the individual populations of centrals (*top*) and satellites (*bottom*) are consistent with

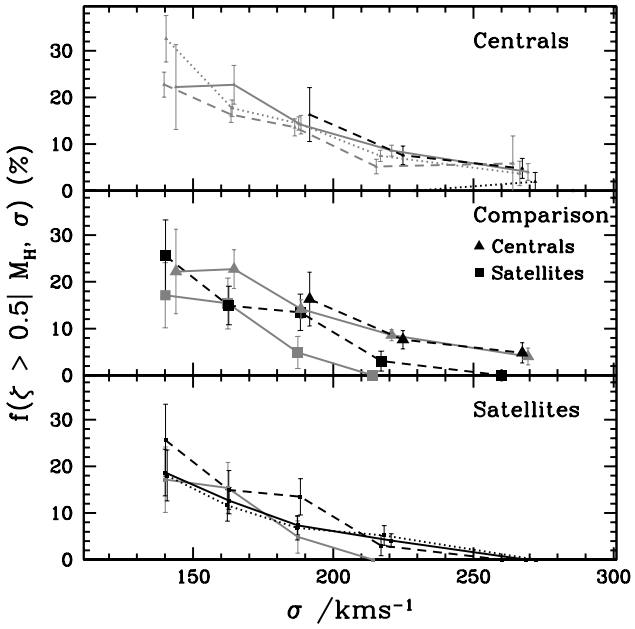

Figure 9. Comparison of the distribution of central and satellite populations with respect to the fraction of galaxies with a ζ value above 0.5, which is consistent with recent star formation. The fraction is conditional i.e. calculated for each bin separately.. The binning with respect to halo mass is the same as in figure 8.

those found in the sample as a whole (see figure 5). However a comparison of the fraction of high ζ values between both centrals and satellites (*middle*) shows a significant difference. The central galaxy data (triangles) are consistently positioned at higher fractions of recent star formation even within the same halo mass range. This might not be particularly surprising: while satellites generally have their accretion of material stopped when they enter the halo, centrals do not, and so can still accrete gas. This mechanism is consistent with the scenario of Kaviraj et al. (2009) and Rogers et al. (2009), whereby the recent star formation seen in elliptical galaxies is fuelled by the accretion of small clouds of gas or satellites,

3.5 Effects with Halo-Centric Radius

Since there is evidence to suggest that the younger low halo mass galaxies are accreted as satellites, we might expect to see younger galaxies on the outskirts of groups. There is also the possibility that the halo-centric radius modulates the efficiency of environmental mechanisms. We investigate this aspect by looking at the relationship of η and ζ as a function of the projected distance from the luminosity weighted centre of the group.

Shown in the right hand panel of figure 10 are the satellite galaxies split into subsamples according to velocity dispersion and halo centric radius, (see fig. 2), against the average values of η for each bin. Since we are looking at galaxies across all group halo masses, the projected distance is scaled using the virial radius of the occupied halo. As found by previous work (e.g. van den Bosch et al. 2008a; Weinmann et al. 2009) there is no significant trend. There is some indication that a reduction in the scatter (bottom panel) of the η values is seen for decreasing radii, although the effect is obviously far from robust. We note that this analysis is complicated both due to the degenerate nature of the projected distance as well as to the fact that smaller halos tend to be more concentrated. These effects are likely to blur the subtle relationships associated with elliptical galaxies and environment.

We also analyse in the left hand panel of figure 10 the conditional fractions of galaxies which have $\zeta \geqslant 0.5$ as a function of the scaled projected distance from the luminosity weighted centre. An inspection of the figure indicates a general trend of increasing recent star formation fractions with projected radius, consistent with the previous comparison of centrals and satellites. The stripping of a satellite surrounding gas may well explain both the trend seen here and in figure 9. Note that the recent star formation fractions seen at the outskirts of the groups are higher than those for the general satellite sample at the same stellar mass. This is consistent with the results seen in Ferreras et al. (2006); Rogers et al. (2007); and Rogers et al. (2009), where we show that galaxies in medium density environments show increased fractions of recent star formation possibly due to interactions. The large error bars are a function of the small numbers which exist away from the group centres, yet the trend is consistent across all mass bins.

To conclude, we find that the effects with halo centric distance are seen mainly in terms of ζ i.e. younger subpopulations. As a result of being accreted into the halo an elliptical galaxy will have any residual star formation halted. On the other hand, we find that the average age of the bulk of the stellar component does not depend on the distance from the centre of the halo. This is to be expected if, as argued by van den Bosch et al. (2008a), a large fraction of early-type galaxies transition onto the red sequence as centrals. It may be that the main effects expected are better analysed within cluster samples (e.g. Nelan et al. 2005).

4 DISCUSSION AND CONCLUSIONS

Using the large $\sim$7,000 strong sample of early-type galaxies described in Rogers et al. (2007) we have investigated the effect of environment, measured through the mass of the dark matter halo that hosts each galaxy. We make use of the previously derived PCA rotated projections, η and ζ, sensitive to the average properties and recent star formation, respectively, to identify small differences in their stellar populations. We find that the star formation histories are mainly a function of velocity dispersion. This is shown in figure 3 where a considerable difference is evident between the effects of velocity dispersion and group halo mass. When we separate out the sample to remove the mass-environment degeneracy, the stellar populations across most of the halos are indistinguishable. Therefore, while the majority of this paper has focused on the small differences observed in the elliptical galaxy population, the main conclusion is that the effect of environment on the stellar populations of early-type galaxies is *extremely limited*. However, we do find that small but nonetheless interesting differences can be detected with respect to environment.

First of all, galaxies within halos with the lowest masses are estimated to be $\sim$1 Gyr younger than those in the rest of the sample. This offset is consistent with the fact that galaxies in low mass halos are exclusively centrals. Thus, they represent the lower end of the environmental density scale and so our result compares favourably with the general view that galaxies in low density regions are $1-2$ Gyr younger (Bernardi et al. 1998; Thomas et al. 2005; Bernardi et al. 2006; Sánchez-Blázquez et al. 2006).

We use in this paper a catalogue of groups to estimate the dark matter halo masses, allowing us to compare more naturally

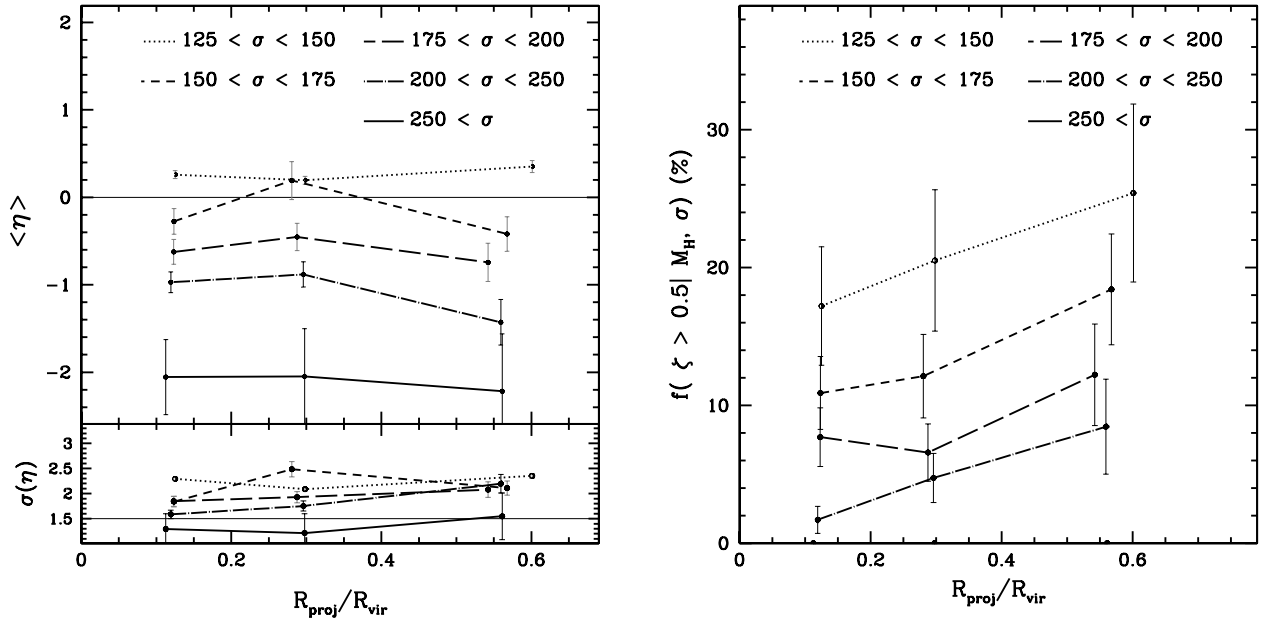

Figure 10. The η and ζ components for the satellite subsample are shown as a function of distance from the luminosity weighted centre of the galaxy group, where the distance is scaled using R_{vir}. (*Left:*) The main panel shows the average η per bin in R_{proj}/R_{vir}, where adjoined points correspond to the same range in velocity dispersion (labelled in km/s). The smaller panel below shows the standard deviation within each bin. (*Right:*) Fraction of galaxies with a ζ value above 0.5 (i.e. those with signatures of recent star formation). The fraction is computed within each bin separately. The error bars are the fractional Poisson errors.

with theoretical modelling results. One of the more recent discoveries is that many observations (e.g. Binney 2004; Croton et al. 2005; Dekel & Birnboim 2006; Cattaneo et al. 2008) can be well explained by assuming a critical halo mass above which the supply of cold gas is stopped by virial shock heating (Birnboim & Dekel 2003; Kereš et al. 2005; Dekel & Birnboim 2006). The critical halo mass is found to be $M_H \sim 10^{12} M_\odot$. Modelling by Cattaneo et al. (2008) show that galaxies above and below this value are consistent with the analysis of Thomas et al. (2005) with respect to galaxies in high/low density regions (see Cattaneo et al. figure 6). It is possible that we see this divide more explicitly here, since the lowest halo bin of this sample is the only one to contain galaxies in halos below or close to the critical mass halo considered here. Our sample gives a consistent $\sim$1 Gyr age difference between galaxies in halos with masses above and below this critical mass. We do not find a gradual trend from the lowest mass halo upwards, a result that may be caused by a combination of effects. The limited timescale of evolutionary signatures on the optical spectra (Harker et al. 2006) and the importance of the individual galaxy mass and the nature of the group build up or the low quality of the data, may mean that the difference in SFH is only visible in the lowest halo mass where the effect is strongest.

The average age is not the only parameter that varies across the sample. The fraction of galaxies with a high value of ζ (consistent with recent star formation) is higher in the four lowest mass halos. The reason for the drop above $M_H \sim 3 \times 10^{13} h^{-1} M_\odot$ is not entirely obvious. However, we note that this is the same halo mass at which a decline is observed in the optical AGN population (Gilmour et al. 2007; Pasquali et al. 2009), possibly giving way to radio-mode AGN. We also note that gas stripping processes are more effective in more massive halos. The modelling results of Simha et al. (2009) indicate that satellites of medium and low mass i.e. those containing the majority of the recent star formation, have their accretion stopped efficiently at halo masses $M_H \sim 10^{14} M_\odot$. We also observe a decrease of recent star formation in the satellite population as a whole, as well as with decreasing halo centric radius, suggesting that such process works across all halo masses although with differing efficiency.

We also investigated the differing effects of environment on the population of central and satellite galaxies. These galaxies are dominant in low and high mass halos, respectively, which implies a limited overlap on the parameter space spanned by M_H and σ. In the range of halo mass over which a comparison is possible, the two populations were found to have similar stellar populations at high velocity dispersion ($\sigma \geqslant$200 km/s). However, at lower values (150 km/s $\leqslant \sigma \leqslant$ 200 km/s), $\langle\eta\rangle$ is higher for satellite galaxies, as expected for younger ages. Hence, the stellar populations of central galaxies were formed earlier. Environmental effects preferentially act on satellites whereas central galaxies mainly move onto the red sequence as the result of a merger or when its halo mass surpasses the critical mass of Dekel & Birnboim (2006). Central galaxies generally sit at the peaks of the dark matter density distribution (Berlind et al. 2003). In halos with mass $M_H \sim 3 \times 10^{13} h^{-1} M_\odot$, centrals are within groups containing significant numbers of additional (satellite) galaxies. Therefore, they are likely to have been subject to a higher level of interactions at earlier times and possibly had gas heated by infalling material and satellites (Khochfar & Ostriker 2008). Furthermore, if we assume that the central galaxy is the core member of the group, we would expect these galaxies to have crossed the threshold of Dekel & Birnboim (2006) earlier than a similar satellite, which would have been accreted later. This would imply that at least *some* satellites will have become ellipticals after being accreted onto the group, creating the lower mean ages. Therefore, we have the emerging picture that while central galaxies are quenched on average at earlier times they retain or accrete small amounts of gas with which to form small amounts of stars.

ACKNOWLEDGMENTS

We would like to thank the referee, Sadegh Khochfar, for his useful comments and suggestions. BR gratefully acknowledges funding from the RAS. SK was supported by a Research Fellowship from the Royal Commission for the Exhibition of 1851. We acknowledge use of the Delos computer cluster at King's College London-Physics. This work makes use of the Sloan Digital Sky Survey. Funding for the SDSS and SDSS-II has been provided by the Alfred P. Sloan Foundation, the Participating Institutions, the National Science Foundation, the U.S. Department of Energy, the National Aeronautics and Space Administration, the Japanese Monbukagakusho, the Max Planck Society, and the Higher Education Funding Council for England. The SDSS Web Site is http://www.sdss.org/. The SDSS is managed by the Astrophysical Research Consortium for the Participating Institutions.

REFERENCES

Adelman-McCarthy, J. K., et al. 2006, ApJS, 162, 38
Barnes,J.E., Hernquist, L., 1996, ApJ, 471 115.
Bell, E. F., et al. 2004, ApJ, 608, 752
Berlind, A. A., et al., 2003, ApJ, 593, 1
Bernardi, M., et al. 1998, ApJ, 508, 143
Bernardi, M., et al. 2003, AJ, 125, 1866
Bernardi, M., et al. 2006, AJ, 131, 1288
Bernardi, M., et al. 2009, MNRAS, 395, 1491
Bezanson, R., et al., 2009, ApJ, 697, 1290
Binney, J., 2004, MNRAS, 347, 1093
Birnboim, Y., Dekel, A., 2003, MNRAS, 345, 349
Blanton, M. R., Eisenstein, D., Hogg, D. W., Schlegel, D. J., & Brinkmann, J., 2005, ApJ, 629, 143
Blanton, M. R., Berlind, A. A., 2007, ApJ, 664, 791
Blanton, M. R., et al. 2005, AJ, 125, 2562
Bovy, J., Hogg, David W., Moustakas, J., 2008, ApJ, 688, 198
Bruzual, G., Charlot, S., 2003, MNRAS, 344, 1000
Cattaneo, A., Dekel, A., Faber, S.M., Guiderdoni, B., 2008, MNRAS, 389, 567
Chabrier G., 2003, PASP, 115, 763
Clemens, M.S., et al. 2006, MNRAS, 370, 702
Cowie, L. L., Songaila, A., Hu, E. M. & Cohen, J. G., 1996, AJ, 112, 839
Croton D. et al. 2005, MNRAS, 365, 11
Dekel, A., Birnboim, Y., 2006, MNRAS, 368, 2
De Lucia G., Springel V., White S. D. M., Croton D., Kauffmann G., 2006, MNRAS, 366, 499
di Matteo, P., Combes, F., Melchior, A.-L., Semelin, B., 2007, A&A, 468, 61
Dressler, A. ApJ, 236, 351, 1980
Faber, S.M., et al. 2007, ApJ, 665, 265
Ferreras, I., Pasquali, A., de Carvalho, R. R., de la Rosa, I. G., Lahav, O., 2006, MNRAS, 370, 828
Fitzpatrick, E. L., 1999 PASP, 111, 63
Folkes, S.R., Lahav, O., Maddox, S. J., 1996, MNRAS, 283, 651
Fontanot, F., et al., 2009, MNRAS, 397, 1776
Gallazzi, A., Charlot, S., Brinchmann, J., White S.D.M., Tremonti, C. A., 2005, MNRAS, 362, 41
Gallazzi, A., et al. 2006, MNRAS, 370, 1106
Gebhardt, K., et al. 2000, ApJ, 539, 13
Gilmour, R., et al., 2007, MNRAS, 380, 1467
Gonzalez, J. J., 1993, Ph.D. thesis, Univ. California, Santa Cruz
Goto T., et al. 2003, AAS, 203, 2602
Gottlöber, S., Klypin, A., Kravtsov, A. V., 2001, ApJ, 546, 223
Harker J.J., Shiavon, R., Weiner, B., Faber, S. 2006, ApJ, 647,103
Hopkins, P.F., et al., 2006, ApJS, 163, 50
Kaviraj, S. et al., 2007, ApJS, 173, 619
Kaviraj, S. et al., 2009, MNRAS, 394, 1713
Kang, X., Jing, Y. P., Mo, H. J., Börner, G., 2005, ApJ, 631, 21
Kauffmann G., et al., 2004, MNRAS, 353, 713
Kereš, D., Katz, N., Weinberg, D. H. & Davé, R., 2005, MNRAS, 363, 2
Khochfar, S., Burkert, A., 2003, ApJ, 597, 117
Khochfar, S., Silk, J. 2006, ApJ, 648, L21
Khochfar, S., Ostriker, J.P., 2008, ApJ, 680, 54
Kuntschner, H., et al., 2001 MNRAS, 323, 615
Madgwick, D., et al, 2003, MNRAS, 343, 871
Naab, T., Burkert, A., 2003, ApJ, 597, 893
Naab, T., Khochfar, S., Burkert, A., 2006, ApJ, 636, 81
Navarro, J. F.; Frenk, C. S.; White, S. D. M. 1997, ApJ, 490, 493
Nelan, J. E., et al., 2005, 2005, ApJ, 632, 137
Pasquali, A., van den Bosch, F.C., Mo, H.J., Yang, X., Somerville, R., 2009, MNRAS, 394, 38
Pasquali, A., Gallazzi, A., Fontanot, F., van den Bosch, F.C., De Lucia, G., Mo, H.J., Yang, X., 2009, submitted to MNRAS (arXiv:0912.1853)
Press W. H., Teukolsky S. A., Vetterling W. T., Flannery B. P., 1992, Numerical Recipes in C. Cambridge Univ. Press, Cambridge
Rogers, B.; Ferreras, I.; Lahav, O.; Bernardi, M.; Kaviraj, S; Yi, Sukyoung K., 2007 MNRAS, 382, 750
Rogers, B., Ferreras, I., Kaviraj, S., Pasquali, A., Sarzi, M., 2009, MNRAS,399, 2172
Rogers, B., Ferreras, I., Peletier, R.F., Silk, J., 2009, MNRAS, in press, arXiv0812.2029
Rogers, B., PhD Thesis, King's College London, 2009
Ronen, S., Aragón-Salamanca, A., Lahav, O., 1999, MNRAS, 303, 284
Sánchez-Blázquez, P. Gorgas, J. Cardiel, N. González, J. J.,2006, A&A, 457, 809
Schawinski, K., et al., 2006, ApJ,
Schlegel, D. J., Finkbeiner, D. P., Davis, M., 1998, ApJ, 500, 525
Slonim, N., Somerville, R., Tishby, N., Lahav, O., 2001, MNRAS, 323, 270
Simha, V., et al., 2009, MNRAS, tmp.1179
Somerville, R.S., 2008, MNRAS, 391, 481
Thomas, D., Maraston, C., Bender, R., Mendes de Oliveira, C., 2005, ApJ, 621, 673
Trager S. C., Worthey G., Faber S. M., Burstein D., Gonzalez J. J., 1998, ApJS, 116, 1
Toomre, A., Toomre, J., 1972, ApJ, 178, 623
van den Bosch, F.C., Yang, X., Mo, H. J., 2003, MNRAS, 340,771
van den Bosch, F.C., et al., 2008, arXiv, 0805.0002
van den Bosch, F.C., et al., 2008, MNRAS, 387, 79
Worthey, G., Ottaviani, D.L., 1997, ApJ, 111, 377
W einmann, S.M., van den Bosch, F.C., Yang, X., Mo, H.J., 2006, MNRAS, 366, 2
Weinmann, S.M., er al., 2009, MNRAS, 1213, 1228
Yang, X., Mo, H. J., van den Bosch, F. C., Jing, Y.P., 2005, MNRAS, 356, 1293
Yang, X., Mo, H. J., van den Bosch, F. C., Pasquali, A., Li, C., Barden, M., 2007, ApJ, 671, 153
Yang, X., Mo, H. J., van den Bosch, F. C., 2008, ApJ, 676, 248
York, D.G., et al 2000, AJ, 120, 1579